Influence of compositional complexity on species diffusion behavior in high

entropy solid-solution alloys

Axel Seoane, Diana Farkas\* and Xian-Ming Bai

Department of Materials Science & Engineering,

Virginia Polytechnic Institute and State University,

Blacksburg, VA 24061

**ABSTRACT** 

Detailed comparative molecular dynamics simulations of the diffusion process in a model

quinary equiatomic FeNiCrCoCu FCC alloy are presented. Vacancy assisted diffusion is studied

by a statistical technique obtaining distributions of vacancy formation and migration energy

values. In addition, vacancy migration is simulated using molecular dynamics at high

temperatures and monitoring mean square displacements over time. To assess the role of

compositional complexity, the results are compared to corresponding simulations in each of the

pure individual components of the alloy as well as the corresponding "average atom" potential,

with similar properties to the alloy but no compositional randomness. The comparison shows that

the diffusion kinetics in the random alloy is not slower than in the average atom material or the

average of the components, indicating that compositional fluctuations do not always result in

"sluggish" diffusion. The results are compared with experimental data for self-diffusion in

similar high entropy alloys.

\*Corresponding author. Email: diana@vt.edu (D. Farkas)

1

#### 1. INTRODUCTION

The "high entropy" or "multi principal element alloys" (HEAs) class of metallic materials can exhibit unique mechanical behavior. In particular, compositionally complex alloys with the face-centered cubic (FCC) structure present strength that increases with decreasing temperature while maintaining good ductility [1]. At high temperatures, HEAs still maintain good strength while conventional Inconel and Haynes superalloys soften significantly [2], making HEAs promising candidates for high-temperature applications. "Sluggish", or slow diffusion of alloying elements due to the presence of atomic-scale energy traps [3] has been postulated as possibly responsible cause for many unique properties in HEAs such as the aforementioned mechanical behavior as well as good creep resistance and slow oxidation kinetics [4-7]. Tsai et al. [8] performed the first HEA diffusion couple experiment using CoCrFeMnNi that showed sluggish diffusion with the temperature scale normalized by the melting temperature. However, the existence of sluggish diffusion is subject to much discussion [9-11], as many following studies of the same and different systems have not shown significant sluggish diffusion [12-20]. Instead, others have reported that only interdiffusion is slower [21-25]. It has been claimed that increasing the number of components (and thus the compositional complexity) in the HEA does not necessary yield ever slower diffusion [16, 17, 26]; Rather the choice of components can have a great impact in the diffusivity, such as Mn in the Cantor alloy [11]. Similarly, Jin and co-workers [27] pointed out that diffusion in medium and high entropy alloys strongly depends on specific constituents. Mehta et al. [28] compared the magnitude of interdiffusion coefficients of individual elements in Al-Co-Cr-Fe-Ni-Mn alloys to the interdiffusion coefficients in relevant quinary, quaternary, and ternary solvent-based alloys. Interdiffusion coefficients

were not necessarily lower in FCC Al-Co-Cr-Fe-Ni-Mn alloys; therefore, no sluggish diffusion was observed in this FCC HEA. In a separate paper [29] they reported experimental measurements of chemical and tracer diffusion coefficients and concluded that diffusion was not necessarily sluggish in Al<sub>0.25</sub>CoCrFeNi high-entropy alloy. In a recent review, Dabrowa et al. [30] concluded that there is no experimental evidence which would support the existence of the sluggish diffusion in HEAs on the level of tracer and selfdiffusivities. Nevertheless, they pointed out that our current state of knowledge on the diffusion in HEAs is still far from complete. Although many of the aforementioned studies indicate that sluggish diffusion may not exist in HEAs, some other studies show that sluggish diffusion does exist under certain circumstances. Osetsky and co-workers [31] argued that coupled percolation and composition-dependent barriers for vacancy jumps within different subsystems in medium- and high-entropy alloys can lead to sluggish diffusion. Chen at al. [24] reported interdiffusion results in Al-Co-Cr-Fe-Ni-Ti HEA indicating that the sluggish diffusion effect exists for only some of the components present in the complex alloy. Recently, Daw and Chandross [32] developed and applied several possible criteria for evaluating "sluggishness" in 57 random equimolar alloys. They found that only a small portion of alloys exhibit possible sluggish diffusion. Interestingly, the existence of such sluggish diffusion is not associated with the increasing compositional complexity but is related to lattice mismatch. Therefore, the existence of sluggish diffusion in HEAs is still controversial. There are a few possible reasons for such a controversy. First, no clear comparison standard has been proposed to define whether the diffusion in HEA's is sluggish or not. Many studies have relied on comparison of HEA diffusion with the elemental diffusion of Ni or other components in the FCC structure and other alloy combinations.

Second, comparing different alloys at the same temperature may not be accurate as the vacancy concentration and migration barriers vary for alloys with different melting temperatures. Third, the measured diffusivities in HEAs are outcomes of synergetic effects of compositional complexity, lattice mismatch, and interactions of different alloying elements (the so-called "cocktail" effect [33]). If one effect is more dominant, the sluggish diffusion (if exists) could be turned on or off. Therefore, development of a strategy that can isolate these effects may help us better understand the possible sluggish effect in HEAs.

In the present paper we propose a different method to clearly isolate the effects of compositional complexity in the diffusion behavior of HEAs. Our technique is based on molecular dynamics (MD) simulations of vacancy-assisted atomic jumps in a complex alloy and in a single component "average atom" system that has similar overall properties as the complex alloy. The former has the compositional complexity while the latter does not. A technique to develop interatomic potentials for such a single component "average atom" system has already been proposed by Varvenne and co-workers [34]. Besides studying vacancy formation and migration energies using the static method, we also follow the atomic jumps of a vacancy in a direct way, monitoring the mean square displacements as a function of time. Therefore, we can address the issue of how the compositional complexity influences species diffusion through correlation effects. In the following sections we report the details of our methodology, results for the statistical study of vacancy formation and migration energies, and diffusion results from monitoring mean square displacements in large scale molecular dynamics simulations at various high temperatures. The results are reported for a) each of the alloy components in the pure FCC form, b) the complex quinary HEA system, and c) the corresponding average atom material. The comparison of the three sets of results

clearly isolates the effects of the compositional complexity. Finally, we compare the results with available experimental data for diffusion kinetics in similar alloys.

### 2. METHODS

## 2.1 Interatomic potential for the model HEA

A recently developed EAM (Embedded Atom Method) [35] interatomic potential was used for the HEA simulations [36]. This potential represents highly idealized interactions that were developed to depict some basic trends in the values of significant alloy properties. While these model interactions cannot accurately represent a particular alloy, they are the ideal way of studying trends, indicating how certain material parameters influence the overall properties of HEAs. The potential set used here is for a five-component Fe-Ni-Cr-Co-Cu alloy in an FCC structure characterized by atomic sizes that differ in no more than 3% and is developed to have binary heats of mixing of no more than 0.7 kJ/mole, well within the range of existence of these alloys (-5  $\leq$   $\Delta H_{mix} \leq$  5 kJ/mol) [37]. The parameters used match some basic elastic and thermodynamic properties, as well as the size mismatches of binary FCC mixtures in the Fe-Ni-Cr-Co-Cu system. The method for generating the potential is similar to those used in previous work [38], but is based on FCC phases being stable for all pure components. This is particularly important for the present work, since we aim at comparing diffusion results with the corresponding ones in the pure FCC components. In other words, this requires all pure component potentials to be stable in the FCC structure. For the components that are not experimentally stable in the pure FCC form (e.g., Fe, Cr, Co), first principles calculation data were utilized. The details of the potential are reported in previous work [36]. The most important findings for the perfect lattice equiatomic quinary alloy is that the standard deviation in the individual nearest neighbor bond lengths was found to be in the range of 2% of the lattice parameter. Table 1 reproduces some of the relevant properties calculated for the pure components using this HEA potential, as reported in reference [36]. Some properties of the equiatomic Fe-Ni-Cr-Co-Cu alloy predicted by the HEA potential are listed in Table 2.

	Fe	Ni	Cr	Co	Cu	Average	Std Dev
						Values	
a (Å)	3.56	3.52	3.53	3.55	3.62	3.556	1.1(%)
E <sub>coh</sub> (eV/atom)	4.40	4.45	4.20	4.41	3.54	4.20	9.1(%)
$B (eV/Å^3)$	1.06	1.13	1.00	1.35	0.86	1.08	16.7(%)
$C_{11} \left( eV/Å^3 \right)$	1.19	1.54	1.24	1.65	1.06	1.34	18.6(%)
$C_{12} \left( eV/\mathring{A}^3 \right)$	1.00	0.92	0.88	1.20	0.76	0.95	17.2(%)
$C_{44} \left( eV/\mathring{A}^3 \right)$	0.48	0.78	0.70	0.89	0.48	0.66	27.4(%)
$E_{v}^{f}(eV)$	1.61	1.61	1.41	1.36	1.19	1.44	12.4(%)
$E_{bcc}$ - $E_{fcc}$ (eV)	0.11	0.15	0.10	0.08	0.22	0.13	42.0(%)
$E_{hep}$ - $E_{fcc}$ (eV)	0.01	0.02	0.01	0.01	0.01	0.01	37.3(%)
$T_{m}(K)$	2730	2210	1930	2190	1175	2047	24.8(%)

Table 1: Selected properties predicted by the HEA potential for the pure components in the FCC structure [36].

## 2.2 The Average Atom potential

Ackland and Vitek [39] were among the first to consider the energetics of random alloys in the context of fitting many-body potentials. FCC binaries based on Ag, Au, and Cu were addressed, including the statistical nature of the species concentration. More recently, analytic expressions up to 2nd order moments for multi-species alloys have been derived [40-43]. The opposite route is also possible, namely, using a multi-species interatomic potential, to determine a consistent single-atom interatomic potential representative of a particular random alloy composition. Such a view was explored by Varvenne and co-workers [34] and is referred to as an "average atom potential" (AA). The average atom potential has averaged out all the local compositional and structural fluctuations of the true random alloy. By comparing the material properties computed for the average and actual random alloys, it is possible to isolate the effects of the random compositional fluctuations. Varvenne and coworkers [34] showed that the average atom potential can be quantitatively accurate for a wide range of random alloy properties. Nöring and Curtin [44] studied the finite-temperature thermodynamic properties of the average-atom potential to determine if the average-atom potential can also represent the important finite-temperature properties of the true random alloy. Using a thermodynamic integration approach, they found that the complex alloy's lattice constant as well as elastic constants are well-predicted by the average-atom potential over a wide temperature range. Thus, they concluded that the average-atom potential is a valuable strategy for modeling complex alloys at finite temperatures. Here we utilize an average atom potential corresponding to the equiatomic quinary HEA, derived using their method.

Table 2 shows some basic properties predicted by the average atom potential, compared with the average of the component properties, as well as the properties predicted by the potential for the HEA complex mixture. The data show that the overall properties predicted by the average atom potential are indeed in quantitative agreement with the average results obtained for the HEA alloy, within 10%. For a more complete and relevant comparison, the table includes vacancy formation and migration energies, calculated as part of this work with the method as described in Section 2.3. Note that the HEA has a range of values for the vacancy formation and migration energies (indicated by "±") due to its compositional fluctuations.

	Average of	Random	Average Atom	
	components	HEA	potential	
a (nm)	0.3556	0.3555	0.3554	
E <sub>coh</sub> (eV)	4.20	4.20	4.20	
B (GPa)	173	169	189	
C <sub>11</sub> (GPa)	214.4	224.8	245.3	
C <sub>12</sub> (GPa)	152	140.8	160.8	
C <sub>44</sub> (GPa)	105.6	107.9	107.9	
$E_{v}^{f}(eV)$	1.44	1.42±0.16	1.43	
$E_{v}^{m}(eV)$	0.98	1.03±0.17	1.03	
$T_{m}(K)$	2047	2070	2130	

Table 2: Selected properties predicted by the potential for the HEA mixture, compared with the average of the component properties, as well as the properties predicted by the average atom potential. The "±" ranges shown in vacancy formation and migration energies for the Random HEA are the calculation results over a large number of possible local configurations.

## 2.3 Calculation of vacancy formation and migration energies

We used the LAMMPS molecular dynamics code [45] to obtain three results at 0 K: the vacancy formation energy and migration barrier, and the activation energy for vacancy-mediated self-diffusion in the system. The first is calculated by comparing the digital sample with the energy of the respective sample with one less atom. The digital samples are the five elements in their pure states, the AA and HEA. The vacancy migration barrier was obtained through the Nudged Elastic Band (NEB) method [46] for all cases. The migration barrier calculated from the NEB method will be compared with the dynamic MD simulation that will be described in the next section. The activation energy for self-diffusion can be obtained by adding the vacancy formation energy and the migration barrier, following the same approach used by Daw and Chandross [32]. We do this and compare it with the experimentally measured activation energies in similar HEAs.

Since the vacancy formation energy in the HEA is different at every atomic site, the mean vacancy formation energy was calculated from 5000 different element distributions for each element, 25000 cases total. Similarly, the mean migration energy in the HEA was calculated through the NEB method for each atom type over 5000 different surrounding neighbor jumps to the vacancy, also 25000 cases total. In the cases of pure elements and the AA, only one vacancy formation energy is required for each atom type because the neighbors are the element itself. The same is true for the migration energy of each pure element or the AA calculated using the NEB method.

# 2.4 Direct observation of vacancy migration at high temperatures

The actual diffusion of a vacancy was simulated with a timestep of 1fs in an NPT (constant number of atoms, pressure, and temperature) ensemble using a Nose-Hoover barostat and thermostat [47]. The external pressure was maintained at zero bars. Periodic boundary conditions were employed in all three Cartesian directions. The simulations were performed in a digital sample that contained 5760 atoms before a vacancy was introduced. In order to get statistically meaningful results, five random distributions of the equiatomic elements in the HEA alloy case were tested for each temperature.

The digital samples began at 600 K with one vacancy introduced, the temperature then was risen to 700 K in 1 million steps (1 ns) and held constant for 10 million steps (10 ns) with snapshots taken every 100 thousand steps (0.1 ns). The temperature was then elevated again by another 100 K in 1 ns and held constant for 10 ns. This was repeated until the last temperature held constant was 2000 K. We defined the starting point for counting jumps when the temperature was held constant in order to avoid volume relaxation fluctuations. The tested temperatures for the AA, HEA and pure elements were from 700 – 2000 K with a 100 K interval, with 5 random distributions for the HEA of equiatomic composition. We chose the simulation time so that a total diffusion length of the vacancy was about three lattice parameters. This is similar to the standards used by Daw and Chandross [32]. In addition, we confirmed the linearity of the MSD plots as a function of time, as an indication that the chosen times were adequate.

The diffusion coefficient was calculated by keeping track of the total movement of the atoms as the vacancy moves over time and the use of the equation:

$$D^{sim} = \frac{\langle R^2 \rangle}{6t},\tag{1}$$

where the  $\langle R^2 \rangle$  is the mean square displacement (MSD) over all atoms in the system and is also commonly calculated in MD. In the case of the five different random distributions for the HEA, MSD was obtained for each case and the overall MSD was the average.  $D^{sim}$  is the diffusion coefficient obtained directly from the simulations. To obtain the self-diffusion coefficient,  $D^{sim}$  has to be normalized by the vacancy concentration ( $x_{vc} = \frac{1}{N}$ ) in the system and the equilibrium vacancy concentration, as done in [48]. This work used the vacancy formation energy to estimate the equilibrium vacancy concentration ( $x_{vc}^e = \exp\left(-E_v^f/k_BT\right)$ ). The final self-diffusion coefficient is calculated by

$$D = \chi_{vc}^e D^{sim} / \chi_{vc}. \tag{2}$$

#### 3. RESULTS

## 3.1 Vacancy formation and migration energies

Vacancy formation energies were calculated using the standard molecular statics method for each of the components in their pure forms and HEA as well as the average atom material. The results are shown in Table 3. For completeness, the cohesive energies for each case are also shown, indicating the general trend that the vacancy formation energies are higher for materials of larger cohesive energy values. In particular, the vacancy formation energy obtained for Cu is significantly lower than those for the other four pure components, consistent with its significantly lower cohesive energy. Most importantly, the results show that the vacancy formation energy obtained for the AA (1.43 eV) material is very close to the average of the vacancy formation energies for the five pure components, as given by the rule of mixtures (1.44 eV).

In the case of the complex HEA alloy, there is a distribution of vacancy formation energies since the vacancy formation energy depends on the chemical complexity in the vicinity of the vacancy. For this case, 25000 different vacancy configurations were analyzed as mentioned in Section 2.3. The results are shown in Figure 1, as a probabilistic distribution of various values of the vacancy formation energy. The results in this figure can be fitted to a Gaussian normal distribution, and we obtained that the average vacancy formation energy in the HEA alloy is 1.42 eV with a standard deviation of 0.16 eV. This is included in Table 3 (the summarized results are also included in Table 2), where it is clear that the average value for the HEA is very close to the average of the corresponding pure elements (1.44 eV), using the rule of mixtures. The average value is also very similar to that found for the AA potential (1.43 eV). We conclude that the

average vacancy formation energy in the HEA is the same as that in the AA potential, but it has a statistical variation that can be characterized by a standard deviation of about 10% of the average value.

Element or Material	Cohesive Energy (eV)	Vacancy Formation Energy (eV)	Migration Energy (eV)	Vacancy Formation Energy in HEA (eV)	Migration Energy in HEA (eV)
Fe	4.4	1.61	1.09	1.48±0.14	1.27±0.16
Ni	4.45	1.61	1.28	1.53±0.14	1.12±0.17
Cr	4.2	1.41	0.96	1.42±0.15	0.99±0.17
Co	4.41	1.36	1.03	1.34±0.14	1.07±0.17
Cu	3.54	1.19	0.51	1.32±0.15	0.72±0.16
Average	4.2	1.44	0.98	1.42±0.16	1.03±0.17
AA	4.2	1.43	1.03	-	-
HEA	4.2	-	-	1.42±0.16	1.03±0.17

Table 3. Cohesive energies, and vacancy formation and migration energies for each component in its pure FCC crystal, the AA material, and the HEA alloy. Here "Average" refers to the average of the components. The "±" range for HEA alloy represents the standard deviation obtained from the Gaussian distribution, originated in the various possible configurations of the alloy.

Vacancy migration energies were calculated using the NEB method [46] for each of the components (in both HEA and their pure FCC crystals) and the average atom material, as shown in Table 3. Note that the summarized results are also included in Table 2. We see that, as

expected, in general the vacancy migration energies are higher for materials of higher cohesive energy values, similar as the vacancy formation energies discussed above. Most importantly, the results show that the vacancy migration energy obtained for the AA material is very close to the average of the vacancy migration energies for the pure components, given by the rule of mixtures.

The chemical complexity of the atoms around a vacancy results in a distribution of vacancy migration energies in the HEA, where the vacancy migration energy depends on the nature of the element type jumping to a neighboring site as well as the chemical complexity in the vicinity of the initial and final vacancy positions. In order to obtain this, 25000 different compositional configurations were analyzed, 5000 for each jumping atom type to the vacancy, as discussed in Section 2.3. The results are shown in Figure 2, as probabilistic distributions of the overall vacancy migration energies as well as for individual elements in HEA. The results in this figure can also be fitted to Gaussian normal distributions and we obtain an average value for the migration energy of each of the components in the HEA, as well as the corresponding standard deviation. These values are included in Table 3. The average vacancy migration energy in the HEA alloy is 1.03 eV with a standard deviation of 0.17 eV. This average value is very close to the average of five pure elements (0.98 eV), and the same as that found for the AA potential (1.03 eV). However, the important difference between HEA and the AA potential is that the vacancy migration energy in the HEA alloy has a statistical variation that can be characterized by a standard deviation of around 15% of the average value.

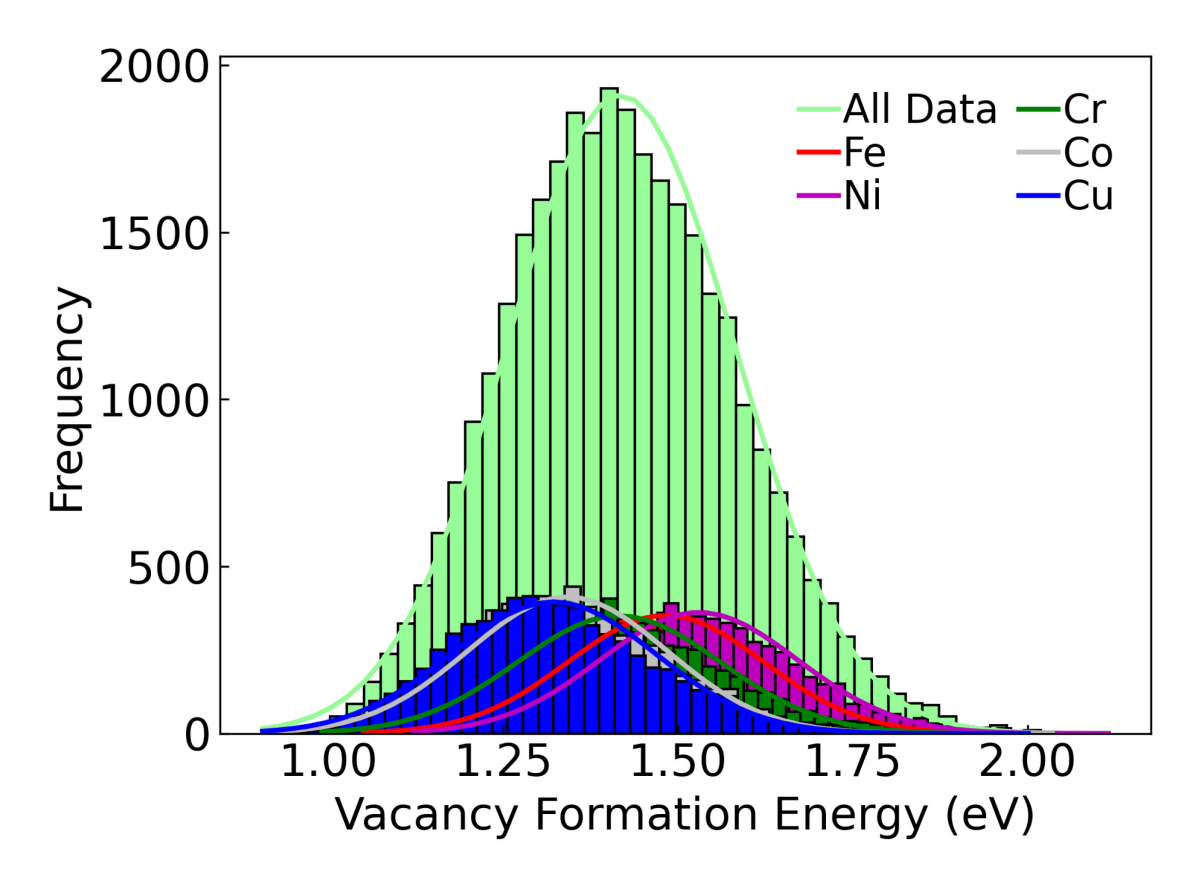


Fig. 1 Distribution of vacancy formation energy values (histograms) found for the HEA, together with fits (lines) to Gaussian normal distributions. The distributions of both total and individual elements are shown.

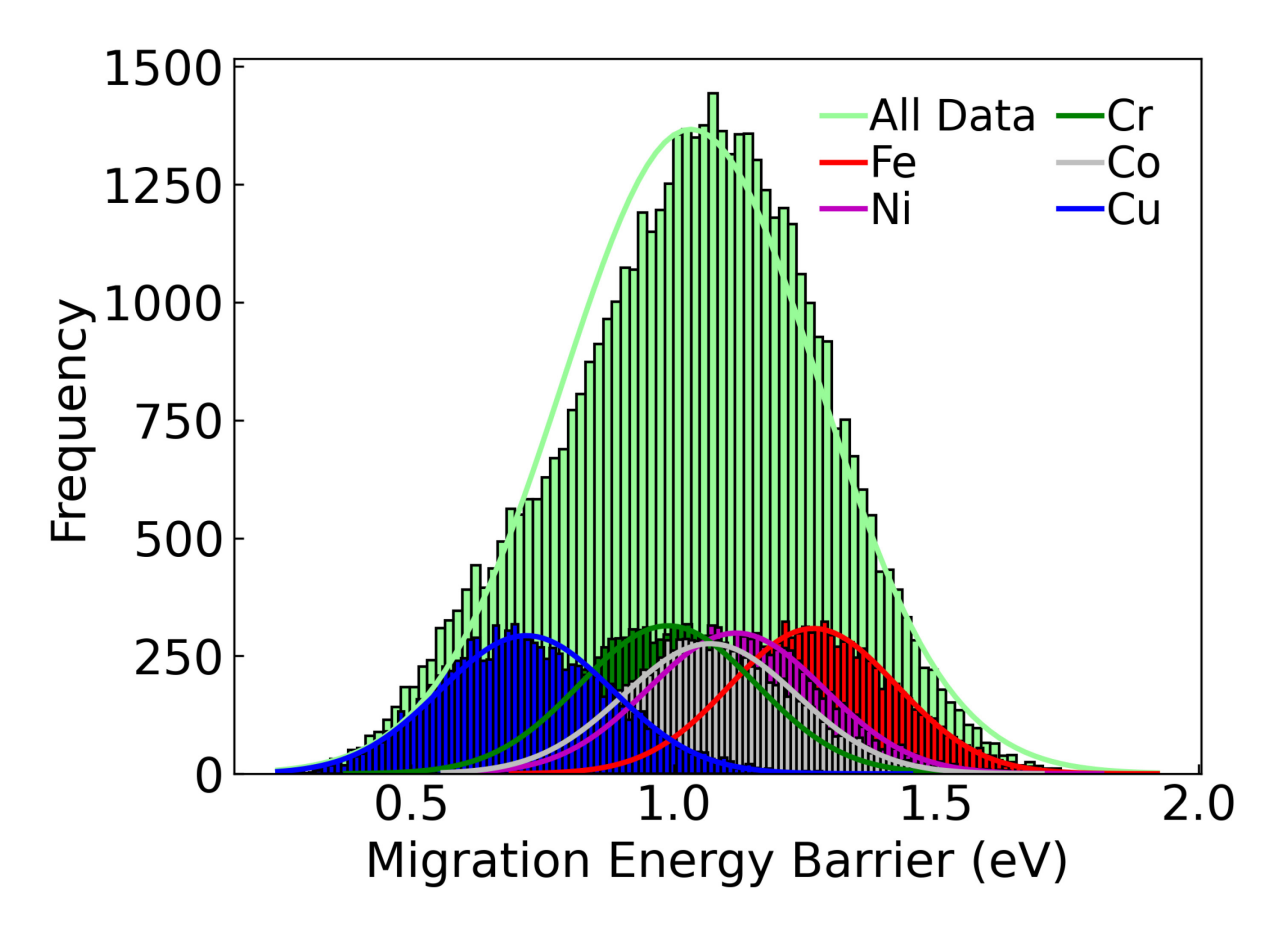


Fig. 2 Distributions of vacancy migration energies (histograms) in the HEA complex alloy, with fits (lines) to Gaussian normal distributions. The distributions of both total and individual elements are shown.

## 3.2 Direct calculations of species diffusivities by MD

To further compare the vacancy migration behavior in different metallic systems, we followed the mean square displacements (MSDs) for all atoms as a function of time in a wide range of temperatures. This was done for each of the five components in their pure crystals, the average atom material, and the complex HEA alloy. For the HEA mixture five different random distributions of the alloying components were considered to understand the role of different random distributions of the component elements on vacancy migration. As expected, the MSDs follow a linear dependence with the simulation time in all cases. Figure 3a shows the MSD results as a function of time for the HEA mixture at different temperatures. Figure 3b shows the

corresponding MSD results for the AA potential at each temperature. There is only one line per temperature as there is only one possible composition for the AA material. These results indicate no sluggish diffusion effect, since for the same temperature, the HEA actually shows greater average displacements than the AA material.

The values for vacancy mobility obtained in this way are taken to be the most accurate to represent the high-temperature dynamics of the system. This is the case even in pure materials where the migration energies obtained from dynamic simulations may not correspond exactly to the calculated values of saddle point energies using the static NEB method. This is even more important for the alloy system, where there is a distribution of migration energies. Following the actual migration of the vacancy at high temperatures is necessary to fully understand the role of compositional complexity.

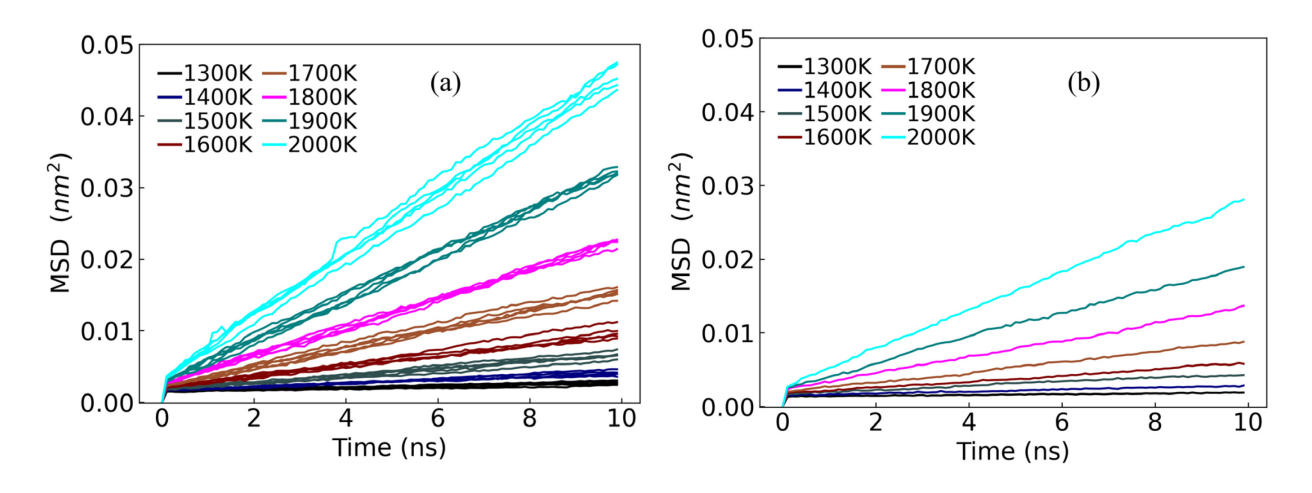


Fig. 3 (a) Mean square displacements (MSDs) of all atoms as a function of time for the HEA complex alloy at different temperatures. At each temperature, the five different lines represent five different atomic configurations in the HEA that were tested to assess the effects of the initial starting configurations. (b) MSDs of all atoms as a function of time for the AA material at different temperatures.

## 3.3 Single element diffusion behavior

In order to obtain the overall or self-diffusivities that can be compared to experiments, the results of following vacancy migration need to be combined with an estimate of the equilibrium vacancy concentration at each temperature. We used the method described in [48] (Eq. (2)). The equilibrium point defect concentration is estimated from the previously calculated vacancy formation energies. For the components in the HEA, their averaged vacancy formation energies are used. In this way we can obtain the Arrhenius plots for overall diffusivities. The results for the five component elements in their pure FCC forms as well as the average atom material are shown in Figure 4a. Figure 4b shows the diffusivity values obtained for each of the components in the HEA complex alloy.

Comparing the results of Figures 4a and 4b, it is clear that Cu diffuses slower in the alloy than when that component is pure. Fe also diffuses slightly slower in HEA while Ni is slightly faster. Yet others (Co, Cr) have diffusivities in the alloy that are similar to those of the pure components. Differences are clearly expected because we have the vacancy migrating in a

different environment. In the case studied here, the most significant effect is seen for Cu. In order to assess the overall effect of the compositional complexity, it is necessary to compare the average diffusivities in the alloy with the averages of the diffusivities of the pure components, or even in a more accurate comparison, with the diffusivity observed in the average atom material. The comparison will be discussed in the next section.

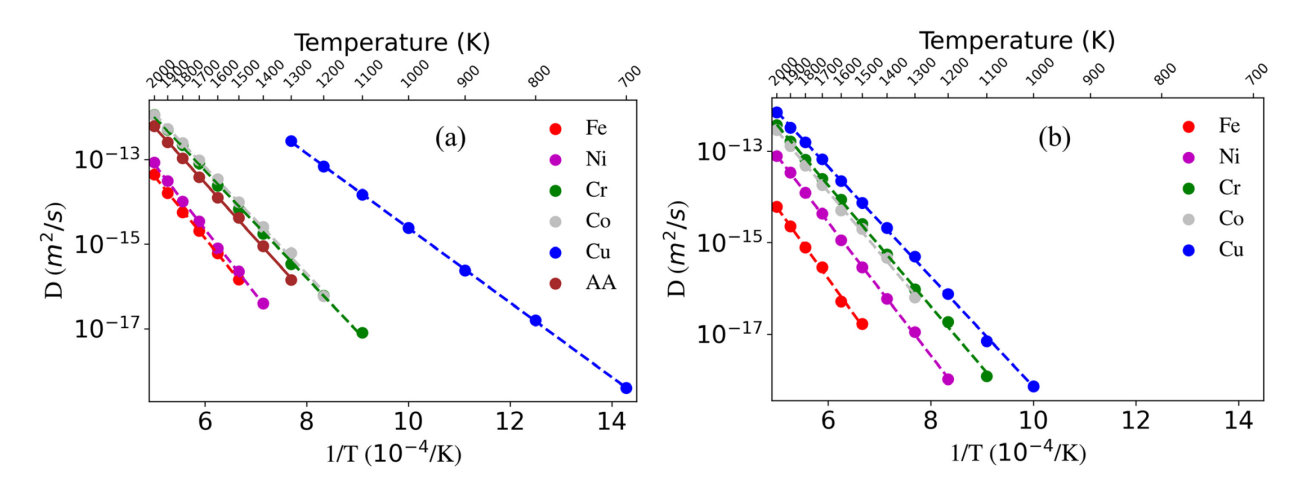


Fig. 4 (a) Arrhenius plots of the diffusivities for all the pure components and the average atom (AA) potential. (b) Arrhenius plots of diffusivities for the individual components in the HEA alloy. Note in both figures the diffusivities are normalized by the thermal vacancy concentration using Eq. (2).

### 3.4 Comparison of diffusion in the HEA, the AA material and the component averages

The comparison of our results for the diffusivities in the complex alloy with those in the average atom material is shown in Figures 5a and 5b. These results are given in the Arrhenius form first with the absolute temperature and then with the homologous temperature (i.e.,  $T/T_m$ ). The error shown in Figure 5 is three times the standard deviation of the 5 diffusivities obtained from the 5 different HEA compositional distributions at each temperature. The comparison clearly indicates that the diffusion behavior in the HEA alloy is remarkably similar to that in the AA material. In particular when the homologous temperature scale is used (Figure 5b), the HEA has almost identical diffusivities with the AA material. Therefore, there is no clear sluggish

diffusion observed for our model HEA. The results demonstrate that the compositional complexity does not imply sluggish diffusion in the equiatomic HEAs, at least for the HEA system and atomic configurations studied here.

Furthermore, a total of three "sluggish diffusion" criteria are evaluated for comparing the diffusion behavior in the HEA with that in pure components, which are also shown in Figures 5a and 5b. These criteria, along with others, were listed in the recent work by Daw and Chandross [32]. The three criteria used here are as follows:

- 1. The arithmetic average of the activation energies (Q) and pre-exponential factors  $(D_0)$ .
- 2. The geometric average of the diffusivities according to the following equation:

$$\langle D \rangle = \left( \prod_{i=1}^{N} D_i \right)^{1/N}. \tag{3}$$

3. The geometric average of the component diffusivities obtained from the Arrhenius relation at the normalized  $T_m/T$  (homologous) temperatures.

The first and second criteria are different applications of the rule of mixtures. The property of an ideal mixture is expected to be the average of the properties of the components. The first criterion averages the activation energies and pre-exponential factors. The second criterion averages the diffusivities geometrically according to Eq. (3). The third criterion accounts for the different equilibrium vacancy concentrations of the components at the same homologous temperatures and avoids the extrapolation beyond the melting point. The melting temperatures (T<sub>m</sub>) used here were the equilibrium temperatures for each system that maintained a stationary solid-liquid interface in an NPT ensemble, which are reported in Tables 1 and 2. Even with these three different criteria, Figure 5 shows that the average diffusivities of the five pure components are very close to that of the HEA, in particular when the comparison is made at the absolute

temperature scale (Figure 5a). When the homologous temperature scale is used (Figure 5b), the HEA shows slight sluggish behavior at low homologous temperatures. However, the difference is relatively small. Therefore, we conclude that overall there is no significant sluggish diffusion effect in our model HEA. This is surprising in spite of the fact that the alloy is made of components characterized by vacancy formation energies that vary by as much as 30% and migration energies that vary by over a factor of 2.

It is also possible to interpret the lack of sluggish diffusion in the complex alloy based on the self-diffusion activation energy, which is the sum of vacancy formation and migration energies. As shown in Table 3, the vacancy formation energies obtained for the complex alloy (here the mean value is used for HEA) and AA material are very similar, and also similar to the prediction of the rules of mixtures based on the values for each of the components. Table 3 also includes the data obtained from a static NEB calculation of vacancy migration energies, and the conclusion is the same: the vacancy migration energies obtained for the complex alloy (here the mean value is used for HEA) and AA material are very similar, and also similar to the prediction of the rules of mixtures based on the values for each of the components. Therefore, the activation energy is similar between the HEA, AA material, and the average of pure components.

We can also compare the vacancy migration energies obtained from the dynamic atomic displacement simulations in different systems. This comparison is shown in Table 4. The results from static NEB calculations are also shown for completeness. The values of the migration energies from the dynamic calculations show the same result: the migration energy obtained for the complex alloy is very similar to that of the AA material, and also similar to the prediction of the rules of mixtures based on the values for each of the pure components. A similar conclusion

can also be obtained using the static NEB results. Again, these comparisons demonstrate that sluggish diffusion may not exist, as least for the model HEA studied in this work.

Element	Migration energy	Migration energy from	
or	from static NEB	Dynamic Diffusion	
Material	Calculation (eV)	Simulation (eV)	
Pure Fe	1.09	1.24	
Pure Ni	1.28	1.62	
Pure Cr	0.96	1.23	
Pure Co	1.03	1.07	
Pure Cu	0.51	0.56	
Average	0.97	1.14	
AA	1.03	1.19	
HEA	1.03	1.17	

 $Table \ 4: Comparison \ of \ vacancy \ migration \ energies \ obtained \ from \ the \ dynamic \ diffusion \ simulations \ as \ well \ as \ those \ calculated \ using \ the \ NEB \ method \ in \ different \ systems.$ 

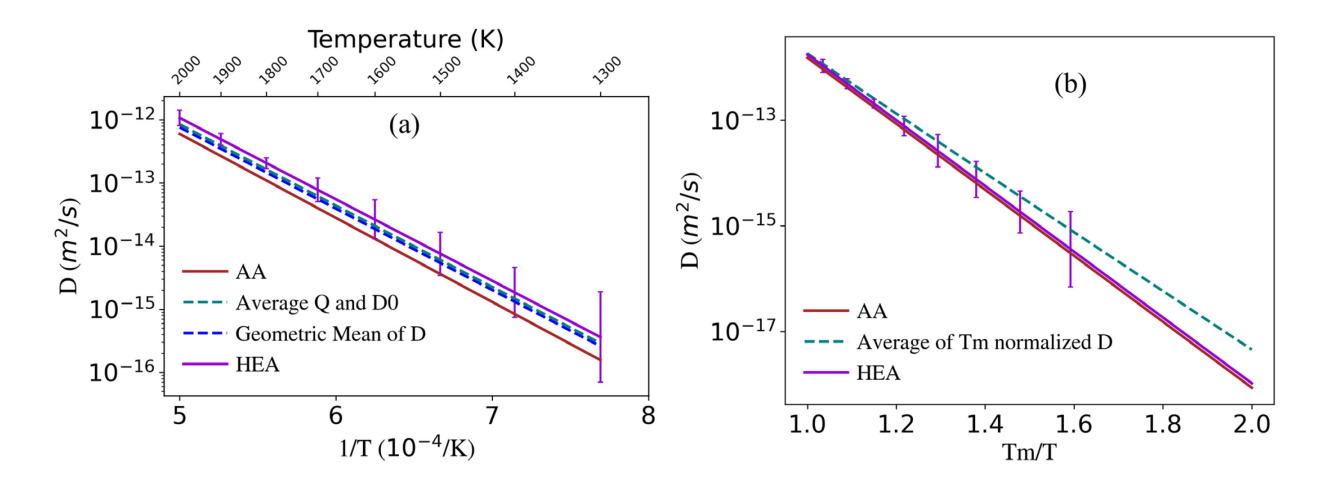


Fig. 5 (a) Comparison of the diffusion behavior in the HEA alloy with that in the AA material as well as the average of the pure components at different absolute temperatures in two criteria: First the average of their individual activation energies (Q) and pre-exponential factors ( $D_0$ ), second the geometric average (Eq. 3) of their extrapolated diffusivity at each temperature. (b) Comparison of the diffusion behavior in the HEA alloy with that in the AA material as well as the average of the pure components at different homologous temperatures ( $T/T_m$ ). The melting temperatures were the temperatures for each system that maintained a stationary solid-liquid interface in NPT. In both figures the error shown is estimated from the five different initial compositional configurations in the HEA.

## 3.5 Comparison with experimental data.

The results shown above for this model HEA indicate that there is no sluggish diffusion effect that can be attributed to the chemical complexity of the alloy. However, the accuracy of the diffusivities reported is only as good as the model interatomic potential utilized. It is therefore important to compare our results for activation energies with experimental values reported in the literature. As mentioned earlier, here the activation energy is the sum of vacancy formation energy and migration energy (for HEA the mean values are used). This is because the experimental self-diffusion activation energy contains both vacancy formation and migration parts. To have a straightforward comparison with the experiments, the unit of activation energies is converted from eV to kJ/mol. This comparison is presented in Table 5. In general, the activation energies from our simulations are slightly lower than their experimental counterparts. Our modeling indicates that the elements with low activation energies in their pure forms (e.g., Cu) tend to increase their activation energies in the HEA, and vice versa (e.g., Ni).

Element	Q in Pure Element Q in HE		Q in Pure Element	Q in Similar HEA	
	(kJ/mol)	(kJ/mol) (kJ/mol)		(kJ/mol)	
	(this work)	(this work)	(Experimental)	(Experimental)	
Fe	261-282	265-298	284 [49]	262-310 [8, 49, 50]	
Ni	279-296	255-279	285 [49]	282-317 [8, 49, 50]	
Cr	227-243	232-253	-	254-309 [8, 49, 50]	
Co	231-242	233-255	288* (HCP) [49]	283-306 [8, 49]	
				_	
Cu	164-169	197-230	210 [51]	147 [18]	

<sup>\*</sup>Pure Co is in the HCP structure in the experimental study.

Table 5: Comparison of our results for the elemental activation energies in pure components and in HEA with available experimental data [8, 10, 18, 49-51]. The lower (higher) bound in the second and third columns is the activation energy obtained by adding the vacancy formation energy and the migration energy obtained from NEB (MD).

### 4. DISCUSSION

This work seeks to determine if this HEA exhibits sluggish diffusion by comparing its diffusion kinetics with the corresponding AA potential as well as the average of the pure elements. The comparison between the AA material and HEA is to isolate the effects of compositional complexity, since many average properties in the two systems are very similar. For example, the vacancy formation energies of these systems are reported in Table 2 and Figure 1 as 1.42 eV for the HEA with a standard deviation of 0.16 eV, an average of 1.44 eV of the corresponding pure elements, and 1.43 eV for the AA potential. Similarly, the vacancy migration barriers of the three systems, calculated with the NEB method, also have similar results, namely: the HEA is 1.03 eV with a standard deviation of 0.17 eV, while the average of the corresponding pure elements is 0.98 eV and for the AA potential it is 1.03 eV. Calculating the migration energies in a dynamic way based on mean square displacements yields the same conclusion: the migration energies are 1.17 eV for the HEA, compared with 1.19 eV for the AA material. All the defect energetic values computed in the present work using the static method point out to the agreement of vacancy formation and migration energies in the alloy with the expected values from the simple arithmetic averaging on the pure components as showed in Table 3. Furthermore, the three different criteria used to average the pure-component results of the kinetic simulations agree closely to the HEA and AA results, as shown in Figure 5. Both methods support the clear conclusion that there is no sluggish diffusion effect that can be attributed to the compositional complexity of the alloy. We note that the migration energies obtained using the dynamic calculation are somewhat higher than those calculated using the NEB method (Table 4). Possible reasons for this discrepancy (e.g., the presence of multiple jumps at high temperatures) were discussed by Lorenzi and Ercolessi [52]. However, Daw and Chandross [32] found good

agreement between both methods in their recent work. Regardless, both methods in this work show no sluggish diffusion effect.

The important difference in vacancy formation and migration energies is that, while the averages are the same, the values obtained for the complex alloy present a statistical distribution. We have found that this distribution can be well represented by a Gaussian normal distribution with a standard deviation of about 15% of the average values. The argument for expecting sluggish diffusion in HEA is the trapping of the diffusing species in low energy configurations. The distribution of values found here indeed includes larger values that can induce trapping effects. However, the distributions that we find also include lower values that may cause the opposite effect, accelerating diffusion. Accelerated vacancy [53, 54] diffusion has been found in dilute alloys. The fact that our distributions are normal in nature may explain why the trapping effects seem to be canceled on average by anti-trapping, accelerating effects by configurations with lower vacancy migration energies. In this work, we have simulated HEA with five random configurations. However, it is possible that some other configurations could still lead to non-Gaussian distributions of vacancy migration and formation energies, and thus result in sluggish diffusion. The search of such configurations can be an interesting future research topic.

Although our results indicate that there is no sluggish diffusion on average, they clearly show that individual components in the alloy can diffuse slower than in the pure component. We find that this is averaged out by other components diffusing faster than in the pure component. This is simply an effect of the vacancy formation and migration process being affected by the different atomic environment in the alloy. The important result of our simulations is that these effects tend to average out when all alloy components in the complex alloy are considered. In the case studied here, Cu is the element that is seen to diffuse slower in the alloy than in its pure FCC

form. This is most likely related to the fact that Cu is the element with lowest vacancy formation and migration energies among all the components. This can also be correlated with the fact that it is the component with the lowest cohesive energy. This effect is balanced in our model HEA alloy by Ni, which diffuses faster in the alloy than that in its pure FCC form. Therefore, if a HEA does not have such balancing elements for cancelling out, the species diffusion in HEA could be slower or faster than the average of pure components. This expectation is consistent with the conclusions in previous experimental studies that some special components may be more important for affecting the overall diffusivity, such as Mn in the Cantor alloy [11].

The results for our dynamic simulations of the individual components in the HEA compare well with independent experimental data in terms of activation energies for vacancy diffusion, as shown in Table 5. The agreement seems reasonable except for Cu. Cu in HEAs is severely understudied [55], with the only data point being [18] where Cu is not a main component but a small solute. In addition to the comparison with available experimental data, our results can be compared to values obtained by first principle techniques such as density functional theory (DFT). There is no previous data on the specific HEA studied in this work, however, the agreement in the pure element cases and similar alloys is encouraging. Mehl and Papaconstantopoulos [56], reported that a vacancy formation energy of 1.18 eV for Cu. Our value of 1.19 eV is in excellent agreement. For Ni, Gong et al. [57] reported values between 1.4 and 1.45 eV and cited several other studies works with values between 1.37 to 1.81 eV. Our value of 1.61 eV is around the average of their cited works. Chen et al. [58] reported the DFT obtained vacancy formation energy of the FCC FeCrCoNi HEA of every element in their pure FCC state and also every element in the HEA. Their pure FCC elemental state results are Fe 1.58, Cr 1.61, Co 1.70 and Ni 1.89 eV. Our values are Fe 1.61, Cr 1.41, Co 1.36 and Ni 1.61 eV.

For their HEA, the values are Fe 1.89, Cr 1.62, Co 1.85 and Ni 1.41 eV. For our HEA they are Fe 1.48, Cr 1.42, Co 1.34 and Ni 1.53 eV. This is a reasonable agreement, given that our HEA composition includes Cu which has a much lower vacancy formation energy than the other elements. For migration energies Angsten et al. [59] reported FCC Fe 1.38, Ni 1.03 and Cu 0.72 eV. Our values are FCC Fe 1.09, Ni 1.28 and Cu 0.51 eV. Overall, the agreement between this modeling work and independent DFT and experimental results is very reasonable, in spite of the fact that the interatomic potentials used here are empirical in nature and are not expected to reproduce precisely the alloy studied. Rather, they are designed to study trends and in the present work they are employed as such.

If the simulation time is long enough, it is possible that atoms may experience some extent of reordering. However, our results do not show any discernible reordering as a result of vacancy diffusion. This was checked by analyzing the local distribution of the elements during the diffusion process. The OVITO [60] visualization software was also used to confirm that no new ordered phases were formed during the process. Unfortunately, the diffusion times we can access are indeed shorter than would be required to observe ordering and we cannot rule out the ordering effects at longer times. In addition, although our times are adequate to study the comparative diffusion behavior, they are also not adequate to study saturation effects of vacancy diffusivity, as observed by Osetsky et al [61].

The lack of the sluggish diffusion should be interpreted in the context of the limitations of the interatomic potential used here for the FeNiCrCoCu HEA. In Section 2.1 we have mentioned that the binary heats of mixing predicted by this potential are less than 0.7 kJ/mole, which is well within the typical range of -5 <  $\Delta H_{mix}$  < 5 kJ/mol for HEA alloys [37]. However, the relatively low heats of mixing make our system close to an ideal solution in terms of the heat

of mixing, possibly affecting the sluggish diffusion effect. Therefore, our observation of the absence of sluggish diffusion does not necessarily extend to systems with non-ideal heats of mixing. Using model interatomic potentials as a representation of such a complex system, clearly has limitations and thus the comparison with the average atom material is critical in providing understanding of the composition complexity effects. It is important to note that even if the potential used here models a nearly ideal solution, the diffusion parameters of the components are widely different, particularly the component Cu presents much lower vacancy formation and migration energies. This variation means that sluggish diffusion can in principle be expected, because the vacancy will follow a local minimum energy path as opposed to a random walk. The important point we make is that it was not observed.

In order to better understand the vacancy migration process, and the reasons why we do not observe sluggish diffusion, we have performed a separate analysis of the total number of atomic jumps observed in a sample of 499 atoms and one vacancy during a 10 ns simulation at various temperatures. A vacancy jump is assumed to occur when an atom moves more than 0.26 nm, which is checked every 100 fs. The results show that the total number of jumps in the HEA is significantly higher than in the AA at all temperatures tested, from 1500K to 2000K. The ratio varies smoothly from about 40% more jumps in the HEA at 2000K to over twice the number of jumps at the lower temperatures. The majority of the observed jumps in the HEA case correspond to Cu atoms jumping into the vacancy. This clearly is related to a complex energy landscape, with lower migration energies for Cu as compared to the other elements. This larger number of total jumps in the HEA counterbalances the expected trapping effects resulting from the vacancy following a local minimum energy path in the HEA instead of the random walk in the AA.

Overall, our results point out to the complexity of the diffusion process in HEA alloys. This complexity has also been pointed out by several other groups. For example, Wang and Wang [62] recently considered the possible range of activation energies for the lattice diffusion in highentropy alloys. Their results highlight the complexity of diffusion pathways in these complex concentrated alloys. Thomas and Patala [63] also pointed out the need to account for the full nature of the energy landscape rather than the migration barrier alone. They concluded that these random landscapes can indeed produce trap environments resulting in sluggish diffusion, but that vacancy diffusion in these complex alloys is not necessarily sluggish. The present results, using the approach of comparing with the average atom case, also indicate that the complexity does not necessarily result in sluggishness.

#### 5. CONCLUSIONS

In this work we proposed an approach for evaluating the existence of sluggish diffusion in the complex equiatomic FeNiCrCoCu model HEA through molecular dynamics simulations. The new approach compares vacancy diffusion for the HEA with that in the corresponding AA (Average Atom) potential, which averages the equilibrium properties of the atoms. We encountered no sluggish diffusion, on average. Comparison with the average diffusion values of the alloy components as inspired by the rule of mixtures also showed no sluggish diffusion overall, with some components diffusing faster and other slower than in the corresponding pure FCC structures. We find that the vacancy formation and migration energies in the HEA alloy present a range of values that can be well represented by a Gaussian normal distribution. This distribution results in a complex energy landscape, including both trapping and antitrapping sites,

whose effects can average out in the alloy. We concluded that this could be one possible reason for why there is no sluggish diffusion in some HEA systems.

### **ACKNOWLEGEMENTS**

The authors acknowledge Advanced Research Computing at Virginia Tech for providing computational resources and technical support that have contributed to the results reported within this paper. URL: <a href="https://arc.vt.edu/">https://arc.vt.edu/</a>. AS acknowledges the support from Virginia Tech's Institute of Critical Technologies and Applied Sciences Doctoral Scholars Program. DF acknowledges support from the National Science Foundation, Grant 1507846. XMB acknowledges the support from the National Science Foundation under Grant No. 1847780.

#### REFERENCES

- [1] B. Gludovatz, A. Hohenwarter, D. Catoor, E.H. Chang, E.P. George, R.O. Ritchie, A fracture-resistant high-entropy alloy for cryogenic applications, Science 345(6201) (2014) 1153-1158.
- [2] Y. Ye, Q. Wang, J. Lu, C. Liu, Y. Yang, High-entropy alloy: challenges and prospects, Materials Today 19(6) (2016) 349-362.
- [3] E. Pickering, N. Jones, High-entropy alloys: a critical assessment of their founding principles and future prospects, International Materials Reviews 61(3) (2016) 183-202.
- [4] G.D. Sathiaraj, P.P. Bhattacharjee, Effect of cold-rolling strain on the evolution of annealing texture of equiatomic CoCrFeMnNi high entropy alloy, Materials Characterization 109 (2015) 189-197.
- [5] C.W. Tsai, Y.L. Chen, M.H. Tsai, J.W. Yeh, T.T. Shun, S.K. Chen, Deformation and annealing behaviors of high-entropy alloy Al0.5CoCrCuFeNi, Journal of Alloys and compounds 486(1-2) (2009) 427-435.
- [6] T. Butler, J. Alfano, R. Martens, M. Weaver, High-temperature oxidation behavior of Al-Co-Cr-Ni-(Fe or Si) multicomponent high-entropy alloys, Jom 67(1) (2015) 246-259.
- [7] D.H. Lee, M.Y. Seok, Y. Zhao, I.C. Choi, J. He, Z. Lu, J.Y. Suh, U. Ramamurty, M. Kawasaki, T.G. Langdon, Spherical nanoindentation creep behavior of nanocrystalline and coarse-grained CoCrFeMnNi high-entropy alloys, Acta Materialia 109 (2016) 314-322.
- [8] K.Y. Tsai, M.H. Tsai, J.W. Yeh, Sluggish diffusion in Co–Cr–Fe–Mn–Ni high-entropy alloys, Acta Materialia 61(13) (2013) 4887-4897.
- [9] S.V. Divinski, A.V. Pokoev, N. Esakkiraja, A. Paul, A mystery of sluggish diffusion in high-entropy alloys: the truth or a myth?, Diffusion Foundations, Trans Tech Publ, 2018, pp. 69-104.
- [10] J. Dąbrowa, M. Danielewski, State-of-the-art diffusion studies in the high entropy alloys, Metals 10(3) (2020) 347.
- [11] J. Dąbrowa, M. Zajusz, W. Kucza, G. Cieślak, K. Berent, T. Czeppe, T. Kulik, M. Danielewski, Demystifying the sluggish diffusion effect in high entropy alloys, Journal of Alloys and Compounds 783 (2019) 193-207.
- [12] J. Dąbrowa, W. Kucza, G. Cieślak, T. Kulik, M. Danielewski, J.-W. Yeh, Interdiffusion in the FCC-structured Al-Co-Cr-Fe-Ni high entropy alloys: experimental studies and numerical simulations, Journal of Alloys and Compounds 674 (2016) 455-462.
- [13] M. Vaidya, S. Trubel, B. Murty, G. Wilde, S.V. Divinski, Ni tracer diffusion in CoCrFeNi and CoCrFeMnNi high entropy alloys, Journal of Alloys and Compounds 688 (2016) 994-1001.
- [14] M. Vaidya, K. Pradeep, B. Murty, G. Wilde, S. Divinski, Radioactive isotopes reveal a non sluggish kinetics of grain boundary diffusion in high entropy alloys, Scientific reports 7(1) (2017) 1-11.
- [15] V. Verma, A. Tripathi, K.N. Kulkarni, On interdiffusion in FeNiCoCrMn high entropy alloy, Journal of Phase Equilibria and Diffusion 38(4) (2017) 445-456.
- [16] C. Zhang, F. Zhang, K. Jin, H. Bei, S. Chen, W. Cao, J. Zhu, D. Lv, Understanding of the elemental diffusion behavior in concentrated solid solution alloys, Journal of Phase Equilibria and Diffusion 38(4) (2017) 434-444.
- [17] M. Vaidya, K. Pradeep, B. Murty, G. Wilde, S. Divinski, Bulk tracer diffusion in CoCrFeNi and CoCrFeMnNi high entropy alloys, Acta Materialia 146 (2018) 211-224.

- [18] D. Gaertner, J. Kottke, G. Wilde, S.V. Divinski, Y. Chumlyakov, Tracer diffusion in single crystalline CoCrFeNi and CoCrFeMnNi high entropy alloys, Journal of Materials Research 33(19) (2018) 3184-3191.
- [19] J. Kottke, M. Laurent-Brocq, A. Fareed, D. Gaertner, L. Perrière, Ł. Rogal, S.V. Divinski, G. Wilde, Tracer diffusion in the Ni–CoCrFeMn system: Transition from a dilute solid solution to a high entropy alloy, Scripta Materialia 159 (2019) 94-98.
- [20] J. Kottke, D. Utt, M. Laurent Brocq, A. Fareed, D. Gaertner, L. Perrière, Ł. Rogal, A. Stukowski, K. Albe, S.V. Divinski, Experimental and theoretical study of tracer diffusion in a series of (CoCrFeMn) 100– xNix alloys, Acta Materialia 194 (2020) 236-248.
- [21] W. Chen, L. Zhang, High-throughput determination of interdiffusion coefficients for Co-Cr-Fe-Mn-Ni high-entropy alloys, Journal of Phase Equilibria and Diffusion 38(4) (2017) 457-465.
- [22] Q. Li, W. Chen, J. Zhong, L. Zhang, Q. Chen, Z.-K. Liu, On sluggish diffusion in fcc Al–Co–Cr–Fe–Ni high-entropy alloys: an experimental and numerical study, Metals 8(1) (2018) 16.
- [23] R. Wang, W. Chen, J. Zhong, L. Zhang, Experimental and numerical studies on the sluggish diffusion in face centered cubic Co-Cr-Cu-Fe-Ni high-entropy alloys, Journal of materials science & technology 34(10) (2018) 1791-1798.
- [24] S.Y. Chen, Q. Li, J. Zhong, F.Z. Xing, L.J. Zhang, On diffusion behaviors in face centered cubic phase of Al-Co-Cr-Fe-Ni-Ti high-entropy superalloys, Journal of Alloys and Compounds 791 (2019) 255-264.
- [25] D. Beke, G. Erdélyi, On the diffusion in high-entropy alloys, Materials Letters 164 (2016) 111-113.
- [26] W. Kucza, J. Dabrowa, G. Cieslak, K. Berent, T. Kulik, M. Danielewski, Studies of "sluggish diffusion" effect in Co-Cr-Fe-Mn-Ni, Co-Cr-Fe-Ni and Co-Fe-Mn-Ni high entropy alloys; determination of tracer diffusivities by combinatorial approach, Journal of Alloys and Compounds 731 (2018) 920-928.
- [27] K. Jin, C. Zhang, F. Zhang, H.B. Bei, Influence of compositional complexity on interdiffusion in Ni-containing concentrated solid-solution alloys, Materials Research Letters 6(5) (2018) 293-299.
- [28] A. Mehta, Y. Sohn, High Entropy and Sluggish Diffusion "Core" Effects in Senary FCC Al-Co-Cr-Fe-Ni-Mn Alloys, Acs Combinatorial Science 22(12) (2020) 757-767.
- [29] A. Mehta, Y. Sohn, Investigation of sluggish diffusion in FCC Al0.25CoCrFeNi highentropy alloy, Materials Research Letters 9(5) (2021) 239-246.
- [30] J. Dabrowa, M. Danielewski, State-of-the-Art Diffusion Studies in the High Entropy Alloys, Metals 10(3) (2020).
- [31] Y.N. Osetsky, L.K. Beland, A.V. Barashev, Y.W. Zhang, On the existence and origin of sluggish diffusion in chemically disordered concentrated alloys, Current Opinion in Solid State & Materials Science 22(3) (2018) 65-74.
- [32] M.S. Daw, M. Chandross, Sluggish diffusion in random equimolar FCC alloys, Physical Review Materials 5(4) (2021) 043603.
- [33] J.W. Yeh, S.K. Chen, S.J. Lin, J.Y. Gan, T.S. Chin, T.T. Shun, C.H. Tsau, S.Y. Chang, Nanostructured high-entropy alloys with multiple principal elements: novel alloy design concepts and outcomes, Advanced Engineering Materials 6(5) (2004) 299-303.
- [34] C. Varvenne, A. Luque, N. W., W.A. Curtin, Average-atom interatomic potential for random alloys, Physical Review B B93 (2016) 104201.
- [35] M.S. Daw, M.I. Baskes, Embedded-Atom Method Derivation and Application to Impurities, Surfaces, and Other Defects in Metals, Physical Review B 29(12) (1984) 6443-6453.

- [36] D. Farkas, A. Caro, Model interatomic potentials and lattice strain in a high-entropy alloy, Journal of Materials Research 33(19) (2018) 3218-3225.
- [37] S. Guo, Q. Hu, C. Ng, C.T. Liu, More than entropy in high-entropy alloys: Forming solid solutions or amorphous phase, Intermetallics 41 (2013) 96-103.
- [38] Y. Mishin, D. Farkas, M.J. Mehl, D.A. Papaconstantopoulos, Interatomic potentials for monoatomic metals from experimental data and ab initio calculations, Physical Review B 59(5) (1999) 3393-3407.
- [39] G.J. Ackland, V. Vitek, Many-body potentials and atomic-scale relaxations in noble-metal alloys, Physical Review B 41(15) (1990) 10324-10333.
- [40] G. Bonny, R.C. Pasianot, L. Malerba, Fitting interatomic potentials consistent with thermodynamics: Fe, Cu, Ni and their alloys, Philosophical Magazine 89(34-36) (2009) 3451-3464.
- [41] D. Terentyev, G. Bonny, C. Domain, R.C. Pasianot, Interaction of a 1/2 < 111 > screw dislocation with Cr precipitates in bcc Fe studied by molecular dynamics, Physical Review B 81(21) (2010).
- [42] G. Bonny, R.C. Pasianot, Gauge transformations to combine multi-component many-body interatomic potentials, Philosophical Magazine Letters 90(8) (2010) 559-563.
- [43] G. Bonny, D. Terentyev, R.C. Pasianot, S. Ponce, A. Bakaev, Interatomic potential to study plasticity in stainless steels: the FeNiCr model alloy, Modelling and Simulation in Materials Science and Engineering 19(8) (2011) 085008.
- [44] W.G. Nöhring, W.A. Curtin, Thermodynamic properties of average-atom interatomic potentials for alloys, Modelling and Simulation in Materials Science and Engineering 24(4) (2016) 045017.
- [45] S. Plimpton, Fast Parallel Algorithms for Short-Range Molecular-Dynamics, J Comput Phys 117(1) (1995) 1-19.
- [46] G. Henkelman, H. Jónsson, Improved tangent estimate in the nudged elastic band method for finding minimum energy paths and saddle points, The Journal of chemical physics 113(22) (2000) 9978-9985.
- [47] G. Bussi, T. Zykova-Timan, M. Parrinello, Isothermal-isobaric molecular dynamics using stochastic velocity rescaling, J Chem Phys 130(7) (2009).
- [48] M.I. Mendelev, Y. Mishin, Molecular dynamics study of self-diffusion in bcc Fe, Physical review B 80(14) (2009) 144111.
- [49] G. Neumann, C. Tuijn, Self-diffusion and impurity diffusion in pure metals: handbook of experimental data, Elsevier2011.
- [50] S. Rothman, L. Nowicki, G. Murch, Self-diffusion in austenitic Fe-Cr-Ni alloys, Journal of Physics F: Metal Physics 10(3) (1980) 383.
- [51] D.B. Butrymowicz, J.R. Manning, M.E. Read, Diffusion in copper and copper alloys. Part I. volume and surface self-diffusion in copper, Journal of Physical and Chemical Reference Data 2(3) (1973) 643-656.
- [52] G.d. Lorenzi, F. Ercolessi, Multiple Jumps and Vacancy Diffusion in a Face-Centered-Cubic Metal, Europhysics Letters (EPL) 20(4) (1992) 349-355.
- [53] I. Belova, G. Murch, Computer simulation of solute-enhanced diffusion kinetics in dilute fcc alloys, Philosophical Magazine 83 (2003) 377 392.
- [54] F. Faupel, D. Hentrich, J. Kluin, J. Wolff, A. Sager, T. Hehenkamp, Diffusion and Vacancy Impurity Interaction in Dilute fcc Alloys, Defect and Diffusion Forum 66-69 (1990) 573 580.

- [55] S. Divinski, O. Lukianova, G. Wilde, A. Dash, N. Esakkiraja, A. Paul, High-entropy alloys: Diffusion, Encyclopedia of Materials: Science and Technology (2020).
- [56] M.J. Mehl, D.A. Papaconstantopoulos, Applications of a tight-binding total-energy method for transition and noble metals: Elastic constants, vacancies, and surfaces of monatomic metals, Physical Review B 54(7) (1996) 4519.
- [57] Y. Gong, B. Grabowski, A. Glensk, F. Körmann, J. Neugebauer, R.C. Reed, Temperature dependence of the Gibbs energy of vacancy formation of fcc Ni, Physical Review B 97(21) (2018) 214106.
- [58] W. Chen, X. Ding, Y. Feng, X. Liu, K. Liu, Z. Lu, D. Li, Y. Li, C. Liu, X.-Q. Chen, Vacancy formation enthalpies of high-entropy FeCoCrNi alloy via first-principles calculations and possible implications to its superior radiation tolerance, Journal of Materials Science & Technology 34(2) (2018) 355-364.
- [59] T. Angsten, T. Mayeshiba, H. Wu, D. Morgan, Elemental vacancy diffusion database from high-throughput first-principles calculations for fcc and hcp structures, New Journal of Physics 16(1) (2014) 015018.
- [60] A. Stukowski, Visualization and analysis of atomistic simulation data with OVITO—the Open Visualization Tool, Modelling and simulation in materials science and engineering 18(1) (2009) 015012.
- [61] Y. Osetsky, A.V. Barashev, Y. Zhang, Sluggish, chemical bias and percolation phenomena in atomic transport by vacancy and interstitial diffusion in NiFe alloys, Current Opinion in Solid State and Materials Science 25(6) (2021) 100961.
- [62] Y.-Z. Wang, Y.-J. Wang, Disentangling diffusion heterogeneity in high-entropy alloys, Acta Materialia 224 (2022) 117527.
- [63] S.L. Thomas, S. Patala, Vacancy diffusion in multi-principal element alloys: The role of chemical disorder in the ordered lattice, Acta Materialia 196 (2020) 144-153.